HHS Public Access
Author manuscript
Science. Author manuscript; available in PMC 2017 November 25.

Directed Evolution of Cytochrome *c* for Carbon–Silicon Bond Formation: Bringing Silicon to Life

S. B. Jennifer Kan[1], **Russell D. Lewis**[1], **Kai Chen**[1], and **Frances H. Arnold**[1,*]

[1]Division of Chemistry and Chemical Engineering, California Institute of Technology, Pasadena, CA 91125, USA

Abstract

Enzymes that catalyze carbon–silicon bond formation are unknown in nature, despite the natural abundance of both elements. Such enzymes would expand the catalytic repertoire of biology, enabling living systems to access chemical space previously only open to synthetic chemistry. We have discovered that heme proteins catalyze the formation of organosilicon compounds under physiological conditions via carbene insertion into silicon–hydrogen bonds. The reaction proceeds both *in vitro* and *in vivo*, accommodating a broad range of substrates with high chemo- and enantioselectivity. Using directed evolution, we enhanced the catalytic function of cytochrome *c* from *Rhodothermus marinus* to achieve more than 15-fold higher turnover than state-of-the-art synthetic catalysts. This carbon–silicon bond-forming biocatalyst offers an environmentally friendly and highly efficient route to producing enantiopure organosilicon molecules.

Silicon constitutes almost 30% of the mass of the Earth's crust, yet no life form is known to have the ability to forge carbon–silicon bonds (1). Despite the absence of organosilicon compounds in the biological world, synthetic chemistry has enabled us to appreciate the unique and desirable properties that have led to their broad applications in chemistry and material science (2, 3). As a biocompatible carbon isostere, silicon can also be used to optimize and repurpose the pharmaceutical properties of bioactive molecules (4, 5).

The natural supply of silicon may be abundant, but sustainable methods for synthesizing organosilicon compounds are not (6–8). Carbon–silicon bond forming methods that introduce silicon motifs to organic molecules enantioselectively rely on multi-step synthetic campaigns to prepare and optimize chiral reagents or catalysts; precious metals are also sometimes needed to achieve the desired activity (9–15). Synthetic methodologies such as carbene insertion into silanes can be rendered enantioselective using chiral transition metal complexes based on rhodium (11, 12), iridium (13) and copper (14, 15). These catalysts can provide optically pure products, but not without limitations: they require halogenated

solvents and sometimes low temperatures to function optimally and have limited turnovers (<100) (16).

Because of their ability to accelerate chemical transformations with exquisite specificity and selectivity, enzymes are increasingly sought after complements to or even replacements for chemical synthesis methods (17, 18). Biocatalysts that are fully genetically encoded and assembled inside of cells are readily tunable using molecular biology techniques. They can be produced at low cost from renewable resources in microbial systems and perform catalysis under mild conditions. Although nature does not use enzymes to form carbon–silicon bonds, the protein machineries of living systems are often "promiscuous", that is, capable of catalyzing reactions distinct from their biological functions. Evolution, natural or in the laboratory, can use these promiscuous functions to generate catalytic novelty (19–21). For example, heme proteins can catalyze a variety of non-natural carbene transfer reactions in aqueous media, including N–H and S–H insertions, which can be greatly enhanced and made exquisitely selective by directed evolution (22–24).

We hypothesized that heme proteins might also catalyze carbene insertion into silicon–hydrogen bonds. Because iron is not known to catalyze this transformation (25), we first examined whether free heme could function as a catalyst in aqueous media. Initial experiments showed that the reaction between phenyldimethylsilane and ethyl 2-diazopropanoate (Me-EDA) in neutral buffer (M9-N minimal medium, pH 7.4) at room temperature gave racemic organosilicon product **3** at very low levels, a total turnover number (TTN) of 4 (Fig. 1A). No product formation was observed in the absence of heme, and the organosilicon product was stable under the reaction conditions.

We next investigated whether heme proteins could catalyze the same carbon–silicon bond-forming reaction. Screening a panel of cytochrome P450 and myoglobin variants, we observed product formation with more turnovers compared to the hemin and hemin with bovine serum albumin (BSA) controls, but with negligible enantioinduction (Table S4). Interestingly, cytochrome *c* from *Rhodothermus marinus* (*Rma* cyt *c*), a gram-negative, thermohalophilic bacterium from submarine hot springs in Iceland (26), catalyzed the reaction with 97% *ee*, indicating the reaction took place in an environment where the protein exerted excellent stereocontrol. Bacterial cytochromes *c* are well-studied, functionally conserved electron-transfer proteins that are not known to have any catalytic function in living systems (27). Other bacterial and eukaryotic cytochrome *c* proteins also catalyzed the reaction, but with lower selectivities. We thus chose *Rma* cyt *c* as the platform for evolving a carbon–silicon bond-forming enzyme.

The crystal structure of wild-type *Rma* cyt *c* (PDB ID: 3CP5; 26) reveals that the heme prosthetic group resides in a hydrophobic pocket, with the iron axially coordinated to a proximal His (H49) and a distal Met (M100), the latter of which is located on a loop (Figs. 1B and 1C). The distal Met, common in cytochrome *c* proteins, is coordinately labile (28, 29). We hypothesized that M100 must be displaced upon iron-carbenoid formation, and that mutation of this amino acid could facilitate formation of this adventitious "active site" and yield an improved carbon–silicon bond-forming biocatalyst. Therefore, a variant library made by site-saturation mutagenesis of M100 was cloned and recombinantly expressed in *E.*

coli. After protein expression, the bacterial cells were heat-treated (75 °C for 10 min) before screening in the presence of phenyldimethylsilane (10 mM), Me-EDA (10 mM) and sodium dithionite ($Na_2S_2O_4$ 10 mM) as a reducing agent, at room temperature under anaerobic conditions. The M100D mutation stood out as highly activating: this first-generation mutant provided chiral organosilicon **3** as a single enantiomer in 550 TTN, a 12-fold improvement over the wild-type protein (Fig. 1D).

Amino acid residues V75 and M103 reside close (within 7Å) to the iron heme center in wild-type *Rma* cyt *c*. Sequential site-saturation mutagenesis at these positions in the M100D mutant led to the discovery of triple mutant V75T M100D M103E, which catalyzed carbon–silicon bond formation in >1500 turnovers and >99% *ee*. This level of activity is more than 15 times the total turnovers reported for the best synthetic catalysts for this class of reaction (16). As stand-alone mutations, both V75T and M103E are activating for wild-type *Rma* cyt *c* and the beneficial effects increase with each combination (Table S5). Comparison of the initial reaction rates established that each round of evolution enhanced the rate: relative to the wild-type protein, the evolved triple mutant catalyzes the reaction >7-fold faster, with turnover frequency (TOF) of 46 min^{-1} (Fig. 1E).

Assaying the new enzyme against a panel of silicon and diazo reagents, we found that the mutations were broadly activating for enantioselective carbon–silicon bond formation. The reaction substrate scope was surveyed using heat-treated lysates of *E. coli* expressing *Rma* cyt *c* V75T M100D M103E under saturating conditions for both silane and diazo ester to determine TTN. Whereas many natural enzymes excel at catalyzing reactions on only their native substrates and little else (especially primary metabolic enzymes), the triple mutant catalyzed the formation of twenty silicon-containing products, most of which were obtained cleanly as single enantiomers, showcasing the broad substrate scope of this reaction using just a single variant of the enzyme (Fig. 2). The reaction accepts both electron-rich and electron-deficient silicon reagents, accommodating a variety of functional groups including ethers, aryl halides, alkyl halides, esters and amides (**5–10**). Silicon reagents based on naphthalenes or heteroarenes (**11–13**) as well as vinyldialkyl- and trialkylsilanes could also serve as silicon donors (**14**, **15**, **18**). In addition, diazo compounds other than Me-EDA could be used for carbon–silicon bond formation (**16**, **17**) (16).

The evolved *Rma* cyt *c* exhibits high specificity for carbon–silicon bond formation. Even in the presence of functional groups that could compete in carbene-transfer reactions, enzymatic carbon–silicon bond formation proceeded with excellent chemoselectivity. For example, styrenyl olefins, electron-rich double bonds, and terminal alkynes that are prime reaction handles for synthetic derivatization are preserved under the reaction conditions, with no competing cyclopropanation or cyclopropenation activity observed. As a result, organosilicon products **12–13** and **18–20** were afforded with 210 to 5010 turnovers and excellent stereoselectivities (98 to >99% *ee*). Preferential carbon–silicon bond formation could also be achieved with substrates bearing free alcohols and primary amines, yielding silicon-containing phenol **21** (910 TTN, >99% *ee*) and aniline **22** (8210 TTN, >99% *ee*). This capability removes the need for functional group protection and/or manipulation, offering a streamlined alternative to transition metal catalysis for incorporating silicon into small molecules. Indeed, when the same reactants were subjected to rhodium catalysis (1

mol% $Rh_2(OAc)_4$), O–H and N–H insertions were the predominant reaction pathways, and copper catalysis (10 mol% $Cu(OTf)_2$) gave complex mixtures of products (Table S7). Tolerance of these highly versatile functionalities in enzymatic carbon–silicon bond-forming reactions provides opportunities for their downstream processing through metabolic engineering, bioorthogonal chemistry, and other synthetic endeavours.

We next asked whether all *Rma* cyt *c* variants would catalyze carbon–silicon bond formation selectively over insertion of the carbene into an N–H bond in the same substrate. We re-visited the evolutionary lineage and tested all four generations of *Rma* cyt *c* (wild-type, M100D, V75T M100D and V75T M100D M103E) with Me-EDA and 4-(dimethylsilyl)aniline (**23**), a reagent that could serve as both nitrogen and silicon donor, to probe the proteins' bond-forming preferences. The wild-type cytochrome *c* in fact exhibited a slight preference for forming amination product **24** over organosilicon product **22**. Even though silane **23** was not used for screening, and the *Rma* cyt *c* therefore never underwent direct selection for chemoselectivity, each round of evolution effected a distinct shift from amination to carbon–silicon bond forming activity (Fig. 3A). This evolutionary path that focused solely on increasing desired product formation culminated in a catalyst that channeled the majority of the reactants (97%) through carbon–silicon bond formation (>30-fold improved with respect to the wild-type), presumably by improving the orientation and binding of the silicon donor.

Some fungi, bacteria and algae have demonstrated promiscuous capacities to derivatize organosilicon molecules when these substances were made available to them (1). The possibility ultimately to establish silicon-based biosynthetic pathways led us to investigate whether the evolved *Rma* cyt *c* could produce organosilicon products *in vivo*. *E. coli* whole cells ($OD_{600} = 15$) expressing *Rma* cyt *c* V75T M100D M103E in glucose-supplemented M9-N buffer were given silane **23** (0.1 mmol) and Me-EDA (0.12 mmol) as neat reagents. The enzyme in this whole-cell system catalyzed carbon–silicon bond formation with 3410 turnovers, yielding organosilicon product **22** in 70% isolated yield (>95% yield based on recovered silane **23**) and 98% *ee* (Fig. 3B). These *in vitro* and *in vivo* examples of carbon–silicon bond formation using an enzyme and earth-abundant iron affirm the notion that nature's protein repertoire is highly evolvable and poised for adaptation: with only a few mutations, existing proteins can be repurposed to efficiently forge chemical bonds not found in biology and grant access to areas of chemical space which living systems have not explored.

Supplementary Material

Refer to Web version on PubMed Central for supplementary material.

Acknowledgments

References and Notes

1. Frampton MB, Zelisko PM. Organosilicon biotechnology. Silicon. 2009; 1:147–163.

2. Rappoport, Z., Apeloig, Y., editors. The Chemistry of Organic Silicon Compounds. Vol. 3. Wiley; 2003.

3. Ponomarenko SA, Kirchmeyer S. Conjugated organosilicon materials for organic electronics and photonics. Adv Polym Sci. 2011; 235:33–110.

4. Showell GA, Mills JS. Chemistry challenges in lead optimization: Silicon isosteres in drug discovery. Drug Discov Today. 2003; 8:551–556. [PubMed: 12821303]

5. Franz AK, Wilson SO. Organosilicon molecules with medicinal applications. J Med Chem. 2013; 56:388–405. [PubMed: 23061607]

6. Anastas, PT., Warner, J. Green Chemistry: Theory and Practice. Oxford Univ Press; New York: 1998.

7. Tondreau AM, Atienza CCH, Weller KJ, Nye SA, Lewis KM, Delis JGP, Chirik PJ. Iron catalysts for selective anti-Markovnikov alkene hydrosilylation using tertiary silanes. Science. 2012; 335:567–570. [PubMed: 22301315]

8. Toutov AA, Liu WB, Betz KN, Fedorov A, Stoltz BM, Grubbs RH. Silylation of C-H bonds in aromatic heterocycles by an Earth-abundant metal catalyst. Nature. 2015; 518:80–84. [PubMed: 25652999]

9. Marciniec, B., editor. Hydrosilylation: A Comprehensive Review on Recent Advances. Springer; Netherlands: 2009.

10. Lee T, Hartwig JF. Rhodium-catalyzed enantioselective silylation of cyclopropyl C–H bonds. Angew Chem Int Ed. 2016; 55:8723–8727. and references therein.

11. Sambasivan R, Ball ZT. Metallopeptides for asymmetric dirhodium catalysis. J Am Chem Soc. 2010; 132:9289–9291. [PubMed: 20518468]

12. Chen D, Zhu DX, Xu MH. Rhodium(I)-catalyzed highly enantioselective insertion of carbenoid into Si–H: Efficient access to functional chiral silanes. J Am Chem Soc. 2016; 138:1498–1501. [PubMed: 26798980]

13. Yasutomi Y, Suematsu H, Katsuki T. Iridium(III)-catalyzed enantioselective Si-H bond insertion and formation of an enantioenriched silicon center. J Am Chem Soc. 2010; 132:4510–4511. [PubMed: 20232868]

14. Zhang YZ, Zhu SF, Wang LX, Zhou QL. Copper-catalyzed highly enantioselective carbenoid insertion into Si-H bonds. Angew Chem Int Ed. 2008; 47:8496–8498.

15. Hyde S, Veliks J, Liégault B, Grassi D, Taillefer M, Gouverneur V. Copper-catalyzed insertion into heteroatom–hydrogen bonds with trifluorodiazoalkanes. Angew Chem Int Ed. 2016; 55:3785–3789.

16. See supplementary materials for details.

17. Bornscheuer UT, Huisman GW, Kazlauskas RJ, Lutz S, Moore JC, Robins K. Engineering the third wave of biocatalysis. Nature. 2012; 485:185–194. [PubMed: 22575958]

18. Tucker JL, Faul MM. Industrial research: Drug companies must adopt green chemistry. Nature. 2016; 534:27–29. [PubMed: 27251259]

19. O'Brien PJ, Herschlag D. Catalytic promiscuity and the evolution of new enzymatic activities. Chem Biol. 1999; 6:R91–R105. [PubMed: 10099128]

20. Copley SD. Enzymes with extra talents: Moonlighting functions and catalytic promiscuity. Curr Opin Chem Biol. 2003; 7:265–272. [PubMed: 12714060]

21. Khersonsky O, Tawfik DS. Enzyme promiscuity: A mechanistic and evolutionary perspective. Annu Rev Biochem. 2010; 79:471–505. [PubMed: 20235827]

22. Coelho PS, Brustad EM, Kannan A, Arnold FH. Olefin cyclopropanation via carbene transfer catalyzed by engineered cytochrome P450 enzymes. Science. 2013; 339:307–310. [PubMed: 23258409]

23. Wang ZJ, Peck NE, Renata H, Arnold FH. Cytochrome P450-catalyzed insertion of carbenoids into N–H bonds. Chem Sci. 2014; 5:598–601. [PubMed: 24490022]

24. Tyagi V, Bonn RB, Fasan R. Intermolecular carbene S-H insertion catalysed by engineered myoglobin-based catalysts. Chem Sci. 2015; 6:2488–2494. [PubMed: 26101581]

25. Only stoichiometric iron carbenoid insertion into Si–H bonds has been reported (*30*)

26. Stelter M, Melo AMP, Pereira MM, Gomes CM, Hreggvidsson GO, Hjorleifsdottir S, Saraiva LM, Teixeira M, Archer M. A novel type of monoheme cytochrome c: Biochemical and structural characterization at 1.23 A resolution of *Rhodothermus marinus* cytochrome c. Biochemistry. 2008; 47:11953–11963. [PubMed: 18855424]

27. Kleingardner JG, Bren KL. Biological significance and applications of heme c proteins and peptides. Acc Chem Res. 2015; 48:1845–1852. [PubMed: 26083801]

28. Levin BD, Walsh KA, Sullivan KK, Bren KL, Elliott SJ. Methionine ligand lability of homologous monoheme cytochromes c. Inorg Chem. 2015; 54:38–46. [PubMed: 25490149]

29. Zaidi S, Hassan MI, Islam A, Ahmad F. The role of key residues in structure, function, and stability of cytochrome-c. Cell Mol Life Sci. 2014; 71:229–255. [PubMed: 23615770]

30. Scharrer E, Brookhart M. Insertion reactions of electrophilic iron carbene complexes with organosilanes: A synthetic and mechanistic study. J Organomet Chem. 1995; 497:61–71.

31. Gibson DG, Young L, Chuang RY, Venter JC, Hutchison CA 3rd, Smith HO. Enzymatic assembly of DNA molecules up to several hundred kilobases. Nat Methods. 2009; 6:343–345. [PubMed: 19363495]

32. Arslan E, Schulz H, Zufferey R, Künzler P, Thöny-Meyer L. Overproduction of the *Bradyrhizobium japonicum* c-type cytochrome subunits of the *cbb*3 oxidase in *Escherichia coli*. Biochem Biophys Res Commun. 1998; 251:744–747. [PubMed: 9790980]

33. Sambrook, J., Frisch, E., Maniatis, T. Molecular Cloning: A Laboratory Manual. Cold Spring Harbor Laboratory Press; New York: 1989.

34. Berry EA, Trumpower BL. Simultaneous determination of hemes *a, b*, and c from pyridine hemochrome spectra. Anal Biochem. 1987; 161:1–15. [PubMed: 3578775]

35. Kille S, Acevedo-Rocha CG, Parra LP, Zhang ZG, Opperman DJ, Reetz MT, Acevedo JP. Reducing codon redundancy and screening effort of combinatorial protein libraries created by saturation mutagenesis. ACS Synth Biol. 2013; 2:83–92. [PubMed: 23656371]

36. Wu J, Panek JS. Total synthesis of (−)-virginiamycin M_2: Application of crotylsilanes accessed by enantioselective Rh(II) or Cu(I) promoted carbenoid Si-H insertion. J Org Chem. 2011; 76:9900–9918. [PubMed: 22070230]

37. Dakin LA, Ong PC, Panek JS, Staples RJ, Stavropoulos P. Speciation and mechanistic studies of chiral copper(I) Schiff base precursors mediating asymmetric carbenoid insertion reactions of diazoacetates into the Si–H bond of silanes. Organometallics. 2000; 19:2896–2908.

38. Dakin LA, Schaus SE, Jacobsen EN, Panek JS. Carbenoid insertions into the silicon– hydrogen bond catalyzed by chiral copper(I) Schiff base complexes. Tetrahedron Lett. 1998; 39:8947–8950.

39. Wang JC, Xu ZJ, Guo Z, Deng QH, Zhou CY, Wan XL, Che CM. Highly enantioselective intermolecular carbene insertion to C-H and Si-H bonds catalyzed by a chiral iridium(III) complex of a D4-symmetric Halterman porphyrin ligand. Chem Commun (Camb). 2012; 48:4299–4301. [PubMed: 22447038]

40. Hrdina R, Guénée L, Moraleda D, Lacour J. Synthesis, structural analysis, and catalytic properties of tetrakis(binaphthyl or octahydrobinaphthyl phosphate) dirhodium(II,II) complexes. Organometallics. 2013; 32:473–479.

41. Ge M, Corey EJ. A method for the catalytic enantioselective synthesis of 6-silylated 2-cyclohexenones. Tetrahedron Lett. 2006; 47:2319–2321.

42. Buck RT, Coe DM, Drysdale MJ, Ferris L, Haigh D, Moody CJ, Pearson ND, Sanghera JB. Asymmetric rhodium carbene insertion into the Si–H bond: Identification of new dirhodium(II) carboxylate catalysts using parallel synthesis techniques. Tetrahedron Asymmetry. 2003; 14:791–816.

43. Buck RT, Coe DM, Drysdale MJ, Moody CJ, Pearson ND. Parallel synthesis techniques in the identification of new chiral dirhodium(II) carboxylates for asymmetric carbenoid insertion reactions. Tetrahedron Lett. 1998; 39:7181–7184. See also reference 47.

44. Doyle MP, Hu W, Phillips IM, Moody CJ, Pepper AG, Slawin AMZ. Reactivity enhancement for chiral dirhodium(II) tetrakis(carboxamidates). Adv Synth Catal. 2001; 343:112–117.

45. Kitagaki S, Kinoshita M, Takeba M, Anada M, Hashimoto S. Enantioselective Si–H insertion of methyl phenyldiazoacetate catalyzed by dirhodium(II) carboxylates incorporating N-phthaloyl-(S)-amino acids as chiral bridging ligands. Tetrahedron Asymmetry. 2000; 11:3855–3859.

46. Davies HML, Hansen T, Rutberg J, Bruzinski PR. Rhodium (II) (S)- N-(arylsulfonyl)prolinate catalyzed asymmetric insertions of vinyl- and phenylcarbenoids into the Si–H bond. Tetrahedron Lett. 1997; 38:1741–1744.

47. Buck RT, Doyle MP, Drysdale MJ, Ferris L, Forbes DC, Haigh D, Moody CJ, Pearson ND, Zhou QL. Asymmetric rhodium carbenoid insertion into the Si–H bond. Tetrahedron Lett. 1996; 37:7631–7634.

48. DeAngelis A, Panish R, Fox JM. Rh-catalyzed intermolecular reactions of α-alkyl-α-diazo carbonyl compounds with selectivity over β-hydride migration. Acc Chem Res. 2016; 49:115–127. [PubMed: 26689221]

49. Wang ZJ, Renata H, Peck NE, Farwell CC, Coelho PS, Arnold FH. Improved cyclopropanation activity of histidine-ligated cytochrome P450 enables the enantioselective formal synthesis of levomilnacipran. Angew Chem Int Ed. 2014; 53:6810–6813.

50. Hyster TK, Farwell CC, Buller AR, McIntosh JA, Arnold FH. Enzyme-controlled nitrogen-atom transfer enables regiodivergent C-H amination. J Am Chem Soc. 2014; 136:15505–15508. [PubMed: 25325618]

51. Coelho PS, Wang ZJ, Ener ME, Baril SA, Kannan A, Arnold FH, Brustad EM. A serine-substituted P450 catalyzes highly efficient carbene transfer to olefins in vivo. Nat Chem Biol. 2013; 9:485–487. [PubMed: 23792734]

52. Renata H, Lewis RD, Sweredoski MJ, Moradian A, Hess S, Wang ZJ, Arnold FH. Identification of mechanism-based inactivation in P450-catalyzed cyclopropanation facilitates engineering of improved enzymes. J Am Chem Soc. 2016; 138:12527–12533. [PubMed: 27573353]

53. Bordeaux M, Tyagi V, Fasan R. Highly diastereoselective and enantioselective olefin cyclopropanation using engineered myoglobin-based catalysts. Angew Chem Int Ed. 2015; 54:1744–1748.

54. Landais Y, Planchenault D. Preparation of optically active alpha-silylcarbonyl compounds using asymmetric alkylation of alpha-silylacetic esters and asymmetric metal-carbene insertion into the Si–H bond. Tetrahedron. 1997; 53:2855–2870.

55. Landais Y, Parra-Rapado L, Planchenault D, Weber V. Mechanism of metal-carbenoid insertion into the Si–H bond. Tetrahedron Lett. 1997; 38:229–232.

56. Peng C, Wang Y, Wang J. Palladium-catalyzed cross-coupling of α-diazocarbonyl compounds with arylboronic acids. J Am Chem Soc. 2008; 130:1566–1567. [PubMed: 18186640]

57. Huang L, Wulff WD. Catalytic asymmetric synthesis of trisubstituted aziridines. J Am Chem Soc. 2011; 133:8892–8895. [PubMed: 21598936]

58. Rayment EJ, Summerhill N, Anderson EA. Synthesis of phenols via fluoride-free oxidation of arylsilanes and arylmethoxysilanes. J Org Chem. 2012; 77:7052–7060. [PubMed: 22866602]

59. Liao WC, Chen WH, Chen CH, Lim TS, Luh TY. Photoinduced electron transfer as a probe for the folding behavior of dimethylsilylene-spaced alternating donor–acceptor oligomers and polymers. Macromolecules. 2013; 46:1305–1311.

60. Oakes FT, Sebastian JF. Direct observation of acyl anion equivalents by carbon-13 Fourier transform Nuclear Magnetic Resonance. J Org Chem. 1980; 45:4959–4961.

61. Rosenberg H, Tsai TT, Ngo NK. Synthesis of carbonate-containing high-temperature poly(arylene-siloxanylenes). J Polym Sci A Polym Chem. 1982; 20:1–13.

62. Dougherty, TK. Aromatic amine terminated silicone monomers, oligomers, and polymers therefrom. US Patent. 5,286,890. 1994.

63. Kim DS, Shim SC. Synthesis and properties of poly(silylenephenylene-vinylene)s. J Polym Sci A Polym Chem. 1999; 37:2263–2273.

64. Wang B, Ma HW, Wang YS, Li Y. Synthesis and characterization of novel liquid crystalline polystyrene. Chem Lett. 2013; 42:915–917.

65. Simonneau A, Oestreich M. 3-Silylated cyclohexa-1,4-dienes as precursors for gaseous hydrosilanes: The B(C$_6$F$_5$)$_3$-catalyzed transfer hydrosilylation of alkenes. Angew Chem Int Ed. 2013; 52:11905–11907.

66. Kisukuri CM, Palmeira DJ, Rodrigues TS, Camargo PHC, Andrade LH. Bimetallic nanoshells as platforms for metallo- and biometallo-catalytic applications. ChemCatChem. 2016; 8:171–179.

67. Denmark SE, Smith RC, Chang WTT, Muhuhi JM. Cross-coupling reactions of aromatic and heteroaromatic silanolates with aromatic and heteroaromatic halides. J Am Chem Soc. 2009; 131:3104–3118. [PubMed: 19199785]
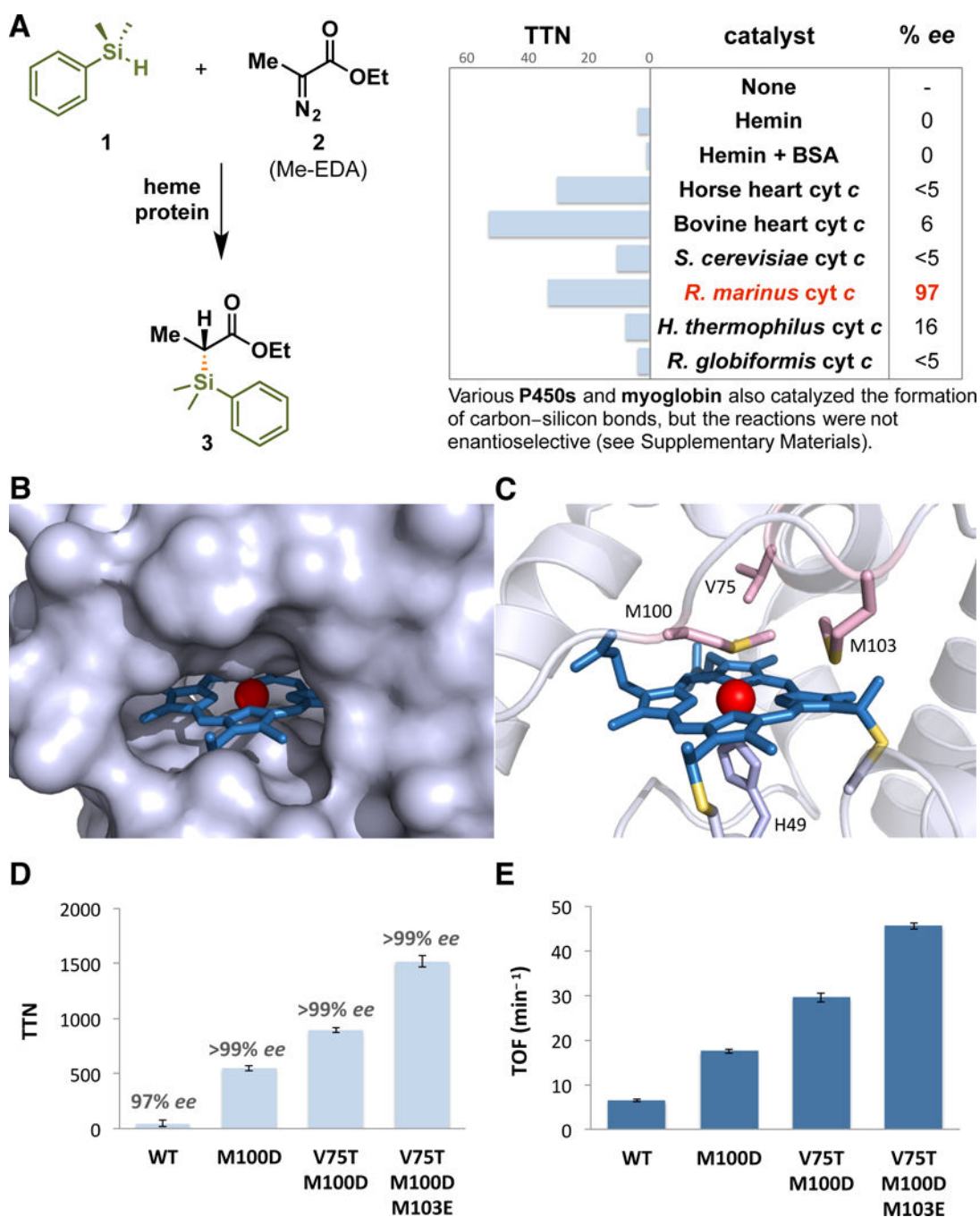
Fig. 1. Heme protein-catalyzed carbon-silicon bond formation
(**A**) Carbon–silicon bond formation catalyzed by heme and purified heme proteins. (**B**) Surface representation of the heme-binding pocket of wild-type *Rma* cyt *c* (PDB ID: 3CP5). (**C**) "Active site" structure of wild-type *Rma* cyt *c* showing a covalently bound heme cofactor ligated by axial ligands H49 and M100. Amino acid residues M100, V75 and M103 residing close to the heme iron were subjected to site-saturation mutagenesis. (**D**) Directed evolution of *Rma* cyt *c* for carbon–silicon bond formation (reaction shown in (**A**)). Experiments were performed using lysates of *E. coli* expressing *Rma* cyt *c* variant (OD_{600} =

15; heat-treated at 75 °C for 10 min), 10 mM silane, 10 mM diazo ester, 10 mM $Na_2S_2O_4$, 5 vol% MeCN, M9-N buffer (pH 7.4) at room temperature under anaerobic conditions for 1.5 h. Reactions performed in triplicate. (**E**) Carbon–silicon bond forming rates over four generations of *Rma* cyt *c*.
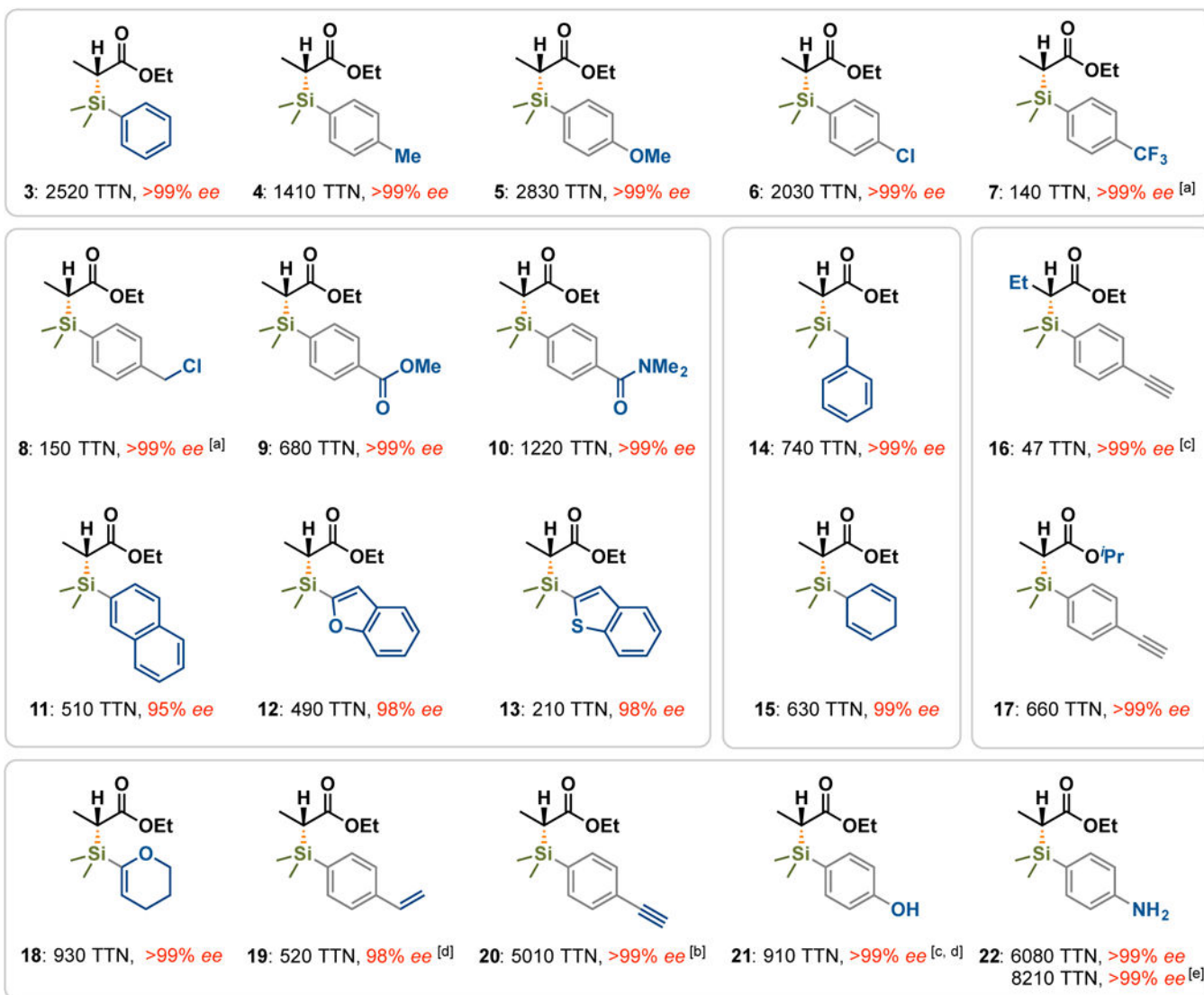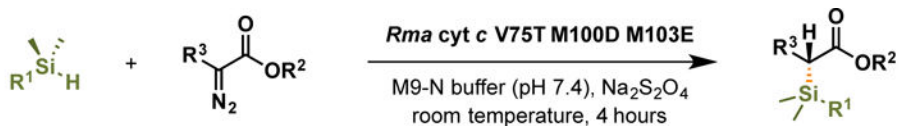
Fig. 2. Scope of *Rma* cyt *c* V75T M100D M103E-catalyzed carbon–silicon bond formation

Standard reaction conditions: lysate of *E. coli* expressing *Rma* cyt *c* V75T M100D M103E (OD$_{600}$ = 1.5; heat-treated at 75 °C for 10 min), 20 mM silane, 10 mM diazo ester, 10 mM Na$_2$S$_2$O$_4$, 5 vol% MeCN, M9-N buffer (pH 7.4) at room temperature under anaerobic conditions. Reactions performed in triplicate. [a] OD$_{600}$ = 5 lysate. [b] OD$_{600}$ = 0.5 lysate. [c] OD$_{600}$ = 15 lysate. [d] 10 mM silane. [e] OD$_{600}$ = 0.15 lysate.
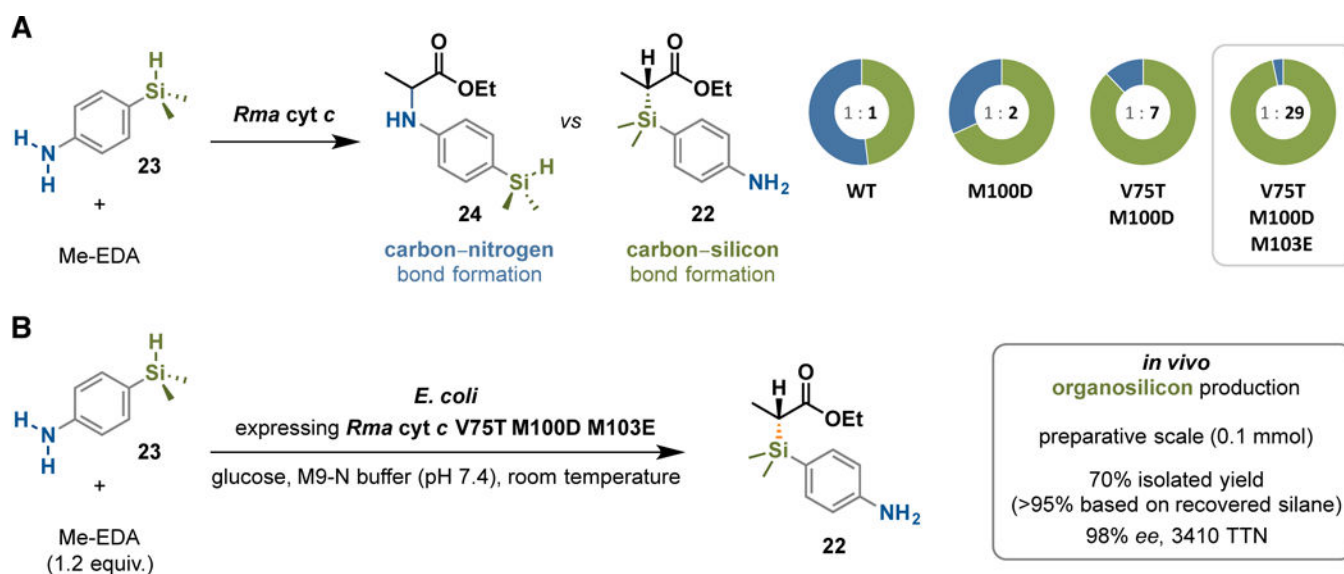
Fig. 3. Chemoselectivity and *in vivo* activity of evolved *Rma* cyt *c*

(A) Chemoselectivity for carbene Si–H insertion over N–H insertion increased dramatically during directed evolution of *Rma* cyt *c*. Standard reaction conditions as described in Fig. 2. Reactions performed in duplicate using heat-treated lysates of *E. coli* expressing *Rma* cyt *c* with protein concentration normalized across variants. Product distribution was quantified after 2 h reaction time (before complete conversion, no double insertion product was observed under these conditions). **(B)** *In vivo* synthesis of organosilicon compound **22**.